Homeotropic Alignment and Director Structures in Thin Films of Triphenylamine-Based Discotic Liquid Crystals Controlled by Supporting Nanostructured Substrates and Surface Confinement

Trirup Dutta Choudhury,[†,‡] Nandiraju V. S. Rao,*[,†] Robert Tenent,[§] Jeffrey Blackburn,[§] Brian Gregg,[§] and Ivan I. Smalyukh[‡,∥,⊥]

Department of Chemistry, Assam University, Silchar-788011, Assam, India; Department of Physics, University of Colorado, Boulder, Colorado 80309, United States; National Renewable Energy Laboratory, 1617 Cole Boulevard, Golden, Colorado 80401, United States; Liquid Crystal Materials Research Center, University of Colorado, Boulder, Colorado, 80309, United States; and Renewable and Sustainable Energy Institute, University of Colorado, Boulder, Colorado 80309, United States

Received: July 9, 2010; Revised Manuscript Received: November 27, 2010

We explore the effects of nanoscale morphology of supporting solid substrates on alignment, defects, and director structures exhibited by thin films of triphenylamine-based discotic liquid crystals. Fluorescence confocal polarizing microscopy and intrinsic polarized fluorescence properties of studied molecules are used to visualize three-dimensional director fields in the liquid crystal films. We demonstrate that, by controlling surface anchoring on supporting or confining solid substrates such as those of carbon nanotube electrodes on glass plates, both uniform homeotropic and in-plane (edge-on) alignment and nonuniform structures with developable domains can be achieved for the same discotic liquid crystal material.

Introduction

During the past few years, the application of π-conjugated liquid crystals (LCs) in organic electronics has attracted much attention in the scientific community because of the self-assembly,[1−3] self-organization,[4] and ease of processing of such soft LC materials. Some of the electronic devices such as light-emitting diodes (LED),[5] photovoltaics (PV),[1,6] field effect transistors (FET),[7−9] sensors,[10] data storage,[11] and others[12] require specially designed soft materials with distinct characteristics of specific molecular alignment and charge transport.[13] The molecular shape and the nature of molecular interactions play an important role in molecular organization and their self-assembly to generate different types of LC phases.[14−17] The rodlike molecules exhibit nematic (orientational order) and smectic (orientational as well as positional order) phases and promote a two-dimensional charge transport in directions perpendicular to the molecular axis. The disk-shaped molecules assemble to organize into columnar (orientational as well as positional order) superstructures and promote one-dimensional charge transport along the columnar axis.[18,19] An extensive study has been performed on the synthesis and properties of the discotic molecules based on the triphenylene and similar kind of aromatic cores, and most of them show columnar phases.[18,19] This type of compound possesses a rigid planar aromatic core with six or eight flexible alkyl chain substituents laterally attached to the core (Figure 1) which provide the solubility and improve the rheology of the LC phase. Discotic liquid crystals (DLC) possess the appropriate molecular design which can be aligned in well-defined, distinct structured layers by different processing techniques essential for effective charge transport.[20−22] The cofacial coupling of π-electrons, resulting from strong intermolecular interactions along these extended aromatic cores in columnar DLC, has been recognized as an efficient structure for charge transport along the columnar axis.[13,23] The fabrication of nanoscale optoelectronic devices is based on the nanostructured one-dimensional (1D) morphology composed of electronically active constituents through $\pi-\pi$ interactions. The sufficiently large planar or nearly planar central aromatic core area in discotic molecules forming columnar mesophases is expected to promote $\pi-\pi$ stacking, thereby enabling efficient intermolecular electronic coupling. Motivated with such a hypothesis, we expected that under tailor-made conditions the strong inherent $\pi-\pi$ stacking in discotic molecules should facilitate their spontaneous assembly into 1D nanofibrils. Hence, the unique disklike structure and its distinct directional electronic charge transport property suggests DLC as potential candidates for applications in molecular electronics and high-efficiency organic photovoltaic devices.[1,24]

Selective infrared excitation of certain vibrational modes of DLC can induce the homeotropic alignment if such an alignment is promoted by an appropriate substrate.[25] Thus, solution processable DLC in combination with a crystal network forming material can lead to stable solid-film structures with useful morphologies for optoelectronic applications such as semiconductor devices.[13] However, the controlled tuning of molecular alignment of the DLC is very important and crucial factor for their application in such devices. The uniaxial planar orientation with the columnar axis parallel to the substrate (edge-on molecular orientation) is the requirement for application in field effect transistors, while the homeotropic alignment with columnar axis perpendicular to the substrate (face-on molecular orientation) is preferred in light-emitting diodes and solar cells.[13] Furthermore, solar cells are fabricated by sequential deposition of organic layers on the anodic substrate followed by vacuum deposition of the cathode. DLCs have some advantages of insensitivity to ionic impurities due to formation of the ordered

* To whom correspondence should be addressed.
[†] Assam University.
[‡] Department of Physics, University of Colorado.
[§] National Renewable Energy Laboratory.
[∥] Liquid Crystal Materials Research Center, University of Colorado.
[⊥] Renewable and Sustainable Energy Institute, University of Colorado.

10.1021/jp106344f
Published on Web 01/07/2011

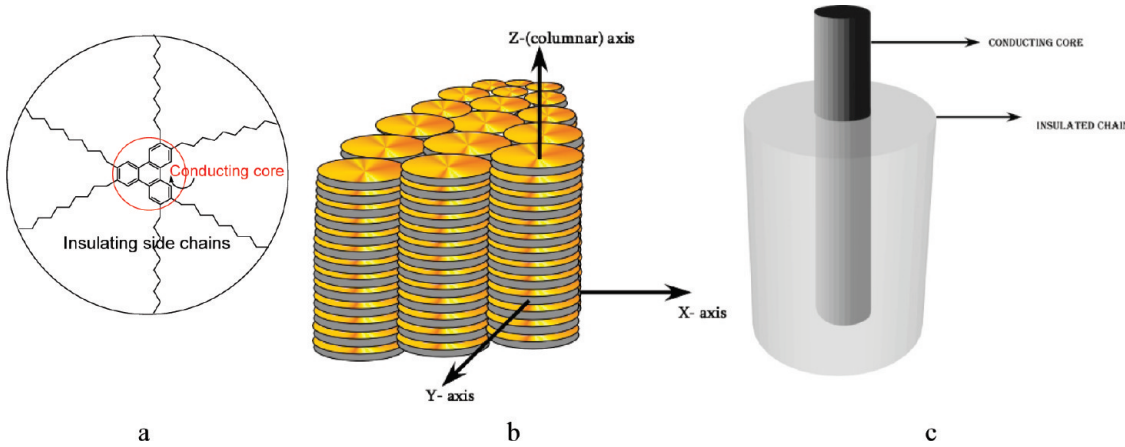

Figure 1. (a) Structure of the triphenylene discotic molecule, (b) two-dimensional molecular arrangement of discotic molecules in a columnar fashion leading to 1D semiconductors along columnar axis, and (c) schematic representation of discotic molecules arranged in columnar fashion as "molecular wires".

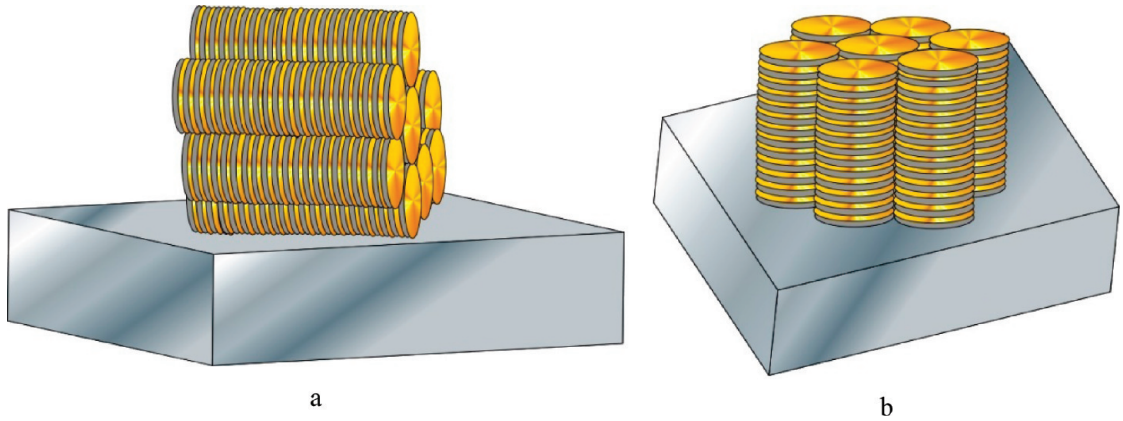

Figure 2. Schematic representation of DLCs: (a) edge-on arranged molecules (planar or homogeneous alignment); (b) face-on arranged molecules (homeotropic alignment).

glassy phase with frozen motion of ions but continuity in migration of the photogenerated charges. However, they suffer from some limitations, including high viscosity due to the bulky alkyl chains and high isotropic clearing temperatures of DLC as a result of the strong intermolecular interactions between the cores.[26]

The homeotropic alignment of discotic columnar mesophases can be induced by different techniques, viz. Langmuir−Blodgett thin films,[27,28] zone-casting technique,[29−31] photopatterning,[32] photoalignment,[33] template growth,[34] magnetic field alignment,[23,35] or lithographically wetting technique.[36] However, a clear understanding about the spontaneous alignment phenomena in absence of external forces is still elusive, even though few reports appeared in literature on hexagonal columnar phases based on interfacial interactions, molecular structure, nature of chemical composition, etc. Systematic studies on discotic molecular alignment[37] in mixtures exhibiting Col_r-Col_h phase variants revealed that the growth of the LC material preferentially starts on the substrate; for a given cooling rate, homeotropic alignment could be kinetically favored for thick films, while stable planar alignment was observed for thin films. A face-on orientation of disks was found to be more favorable at the substrate−LC interface, whereas an edge-on orientation would prevail at the LC−air interface.[38] Hence, any attempt to establish simple and direct processes for the optimal alignment of DLC[23,39] presents an experimental challenge and represents a desirable advance for the scalable application of these materials in optoelectronic applications.

Various device configurations require specific alignment of DLC materials between the electrodes. For example, homogeneous (edge-on) molecular arrangement along the substrate is required for the field effect transistor as depicted in Figure 2a.[38] Such a specific molecular alignment can be accomplished by different processing techniques such as surface treatment, the use of different fields such as electric or magnetic, adjusting the rate of temperature swing (e.g., rapid thermal quenching), etc. In contrast, the main charge transport for photovoltaic cells takes place perpendicular to the substrate and therefore requires homeotropic alignment, viz. face-on molecular arrangement of the discotic molecules with uniaxial orientation along the charge transport direction, as shown in Figure 2b.

In this paper we present results of unique experimental techniques for homeotropic alignment of triphenylamine-based discotic liquid crystal (TPAD-12) based on nanostructured substrates of single-walled carbon nanotubes (SWNTs). The triphenylamine core is similar to that of triphenylene core, but here all the three benzene rings are attached to a central nitrogen atom. This central core is attached to nine flexible alkoxy chains via imine and ester linkage as shown in Figure 3a. The synthesis of the compound was reported earlier, and a fresh sample was synthesized following the same procedure.[40,41] The compound due to nine flexible alkyl chains and the presence of ester and imine linkages in branches make it as an interesting compound for study for its molecular orientational characteristics on different substrates. The space filling of the three wings of the molecule resembles the twisted fan shape.

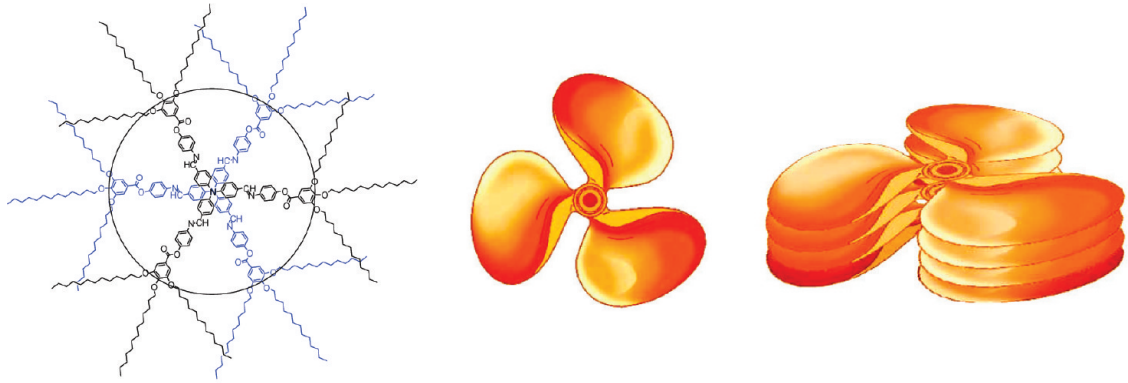

a b c

Figure 3. (a) Molecular structure of triphenylamine-based discotic liquid crystals, (b) fanlike model of the molecular structure, and (c) arrangement of fanlike molecules in the columnar phase.

In order to elucidate the functionalities of these films for their potential applications, a critical examination of molecular organization and surface morphology at nano- and microscale is required.[42−44] The molecular orientation in the liquid crystalline phases is described by the molecular director field, and hence imaging of the three-dimensional (3D) molecular director field structures is necessary for fundamental studies and technological applications of liquid crystals. The 3D molecular structural information can be obtained either from fluorescence confocal polarizing microscopy[45−48] (FCPM) studies in nonfluorescent LC samples doped with anisotropic dye molecules or from coherent anti-Stokes Raman scattering (CARS) polarized microscopy[49−51] in pure LC samples. In the present work FCPM studies were carried out on pure samples to infer the polarization-dependent fluorescence in these compounds since the TPAD-12 sample exhibits anisotropic fluorescence. Further, it was recently demonstrated[52−54] that the regular arrays of toric focal conic domains exhibited by smectic A phase can be confined within surface-modified microsized channels. An experiment carried out to determine the influence of surface anchoring on the alignment of TPAD-12 discotic molecules in microchannel is also discussed.

Experimental Section

The visualization of columnar molecular alignment was carried out on Nikon BX-52 polarizing microscope attached with a hot stage (Instec Inc.). The surface morphology of the compound TPAD-12 was examined on air suspended Nanoscope III Multimode (digital instrument) atomic force microscopy (AFM). Samples were studied using tapping mode, and all the measurements were carried out in air using silicon cantilever (Visa probe) with resonance frequency of ~300 kHz. The scanning range varies from 1 × 1 μm to 10 × 10 μm. To visualize molecular orientation patterns in three dimensions, we have used FCPM built around an inverted IX-71 microscope (Olympus). The excitation beam (488 nm Ar laser) was focused by an objective into a small (<1 μm^3) volume in the sample. An achromatic linear polarization rotator was used to control the polarization of both excitation and detected fluorescent light. Fluorescent light from this volume was detected by a photomultiplier tube after passing through a pinhole and interference filters in the spectral region 510−550 nm. A pinhole (in a focal plane next to the detector) discriminates against the regions above and below the selected volume in the studied sample. The pinhole size was adjusted depending on objective's magnification and numerical aperture (an immersion-oil objective (60×, NA = 1.4) and a dry objective (40×, NA = 0.6). A focused beam scans a sample in horizontal planes at different fixed depths. Coordinate-dependent fluorescence intensity data were stored in the computer memory and then used to compose the sample's cross sections and to reconstruct a fluorescence 3D image (in-plane or vertical cross sections) revealing the patterns of molecular alignment. The magnetic alignment of the compound was done by 2 T electromagnet.

Preparation of Film on Different Substrates. Different types of substrates, viz. untreated and treated glass plates, polyimide (PI) and indium tin oxide (ITO)-coated glass plates, silicon wafer, and SWNT-coated electrodes, were used in this work. Films of different thickness had been prepared by spin-coating using solutions of known concentrations at variable speeds in a 3G spin-coater. For the homeotropic alignment the film was obtained on polyimide, ITO, and SWNT-coated substrates. About 3.7−20 mg of the TPAD-12 was dissolved in 300−500 μL of toluene. The solution was sonicated for 15 min at 60 °C, and then the solution was cooled down to the room temperature. The normal coverslips were first washed with methanol and acetone and then cleaned by plasma cleaning to remove the entire dust and oil particles. After that nitrogen gas was blown over the coverslip, the clean coverslip was then put on the 3G spin-coater, and the TPAD-12 solution was transferred dropwise to cover the whole surface area of the coverslip. Then the spin-coater was rotated at 4000 rpm for 30 s to form a uniform film on the coverslip. A similar procedure was repeated for silicon wafer, ITO-coated glass plate, and SWNT-coated glass plate (nanostructured electrode[55]) which was supplied by National Renewable Energy Laboratory (NREL, Golden, CO). In the case of polyimide-coated film, a clean glass plate was first spin-coated with a layer of polyimide and heated for 2 h at 200 °C and then cooled to room temperature. After that, the solution of TPAD-12 was spin-coated on top of it.

Preparation of SWNT-Coated Electrode. *SWNT Material.* SWNT samples were produced in-house using laser vaporization (LV). The details of methods for soot generation, purification, dispersion, and electrode spray-coating have been previously published.[55]

(a) Raw Material (Soot) Purification. Briefly, ~100 mg of SWNT soot was refluxed in 4 M nitric acid for 18 h. The resulting SWNT slurry was filtered through a 90 mm PTFE filter and washed repeatedly with successive treatment of water and acetone and finally 1 M KOH. The resulting purified buckey-

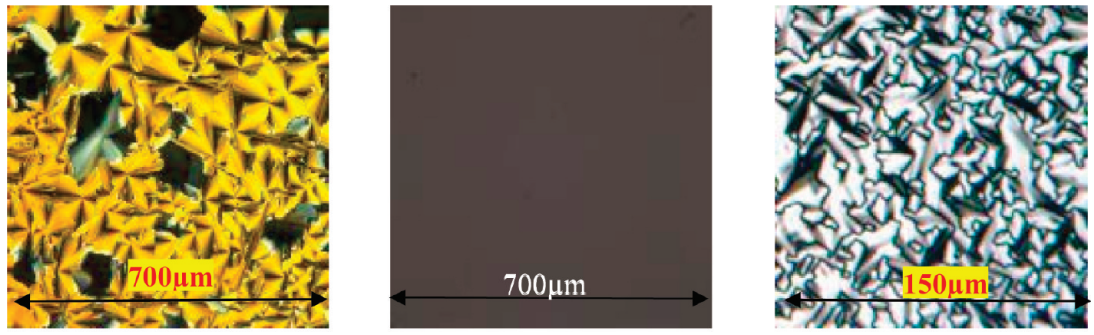

Figure 4. Optical microscopy photographs: (a) normal glass slide, (b) spin-coated sample on ITO glass slide, and (c) optical texture of the spin-coated sample on ITO glass slide after heating to isotropic phase and upon slow cooling to mesophase; thickness is the same as in (b).

paper of SWNTs was burned in air at 525 °C for 1 min to remove amorphous carbon.

(b) Dispersions. 5 mg of purified carbon nanotube paper was added to 20 mL of a 1% CMC solution. This solution was then sonicated for 10 min using a 1/4 in. probe sonicator operated at 225 W (Cole Parmer model CPX 750, 20 kHz). The solution was then centrifuged at 28 000 rpm (~134 000 × 9.81 m/s^2 centrifugal force, maximum) in a SW32Ti rotor (Beckman) for 4 h, and the final dispersion was obtained by decanting the top 80% of the supernatant liquid.

(c) Substrate Materials and Preparation. Films were deposited on 25 mm × 75 mm glass microscope slides purchased from VWR (Cat. No. 48300-036). The substrates were cleaned with an isopropanol-soaked clean room wipe and then placed in an oxygen plasma (800 mTorr, 155 W) for 5 min.

(d) Spraying Conditions. SWNT films were sprayed using a home-built ultrasonic spray system that utilizes a Sono-tek Impact ultrasonic spray nozzle. The SWNT dispersion was pumped to the nozzle at 250 μL/min. The power supplied to the ultrasonic spray head was 2.8 W. Nitrogen flowing at 6.8 SLPM was used to carry the atomized dispersion to the underlying substrate surface. The substrate was heated to 80 °C to aid in drying.

(e) Surfactant Removal and Tube Doping. Samples were placed in 4 M HNO_3 overnight to remove surfactant and dope the networks. After removal from the acid bath, the samples were air-dried and then rinsed by placing them into a bath of deionized water for 30 min.

Magnetic Field Experiment. For magnetic field experiment 6 μm cell was filled by TPAD-12 by capillary action from isotropic melt. The cell was then placed between the pole pieces of an electromagnet (2 T) with an indigenous heater attached with a microcontroller. The cell was heated up to isotropic temperature and then cooled down to room temperature in the presence of magnetic field. The magnetic flux was parallel to the cell because discotic liquid crystals possess large negative diamagnetic anisotropy and hence align in a perpendicular direction to the magnetic field means perpendicular to the substrate.

Microchannel Experiment. The condition for planar and homeotropic alignment of the liquid crystal can be controlled by adsorbing the hydrophilic or hydrophobic material on the substrate or by rubbing to create fine grooves in the surface. The microchannel experiment demonstrated an approach to control the orientation of the liquid crystal by geometric confinement in surface-modified microchannel. By confining the discotic molecules in 20 μm sized rectangular channels with control surface polarity, we were able to generate the defect free domain by slow heating and cooling. Microchannels were fabricated on (100) silicon wafers using photolithography and reactive etching techniques.[56] The microchannel experiment was done on silicon wafer having a fine channel of square cross section with dimensions of 20 μm width, 60 μm depth, and 10 mm long as shown in Figure 6a. The surface polarity of the microchannel was controlled following the chemical cleaning by ultrasonication in a mixture of dimethylformamide (DMF) and methanol to remove chemical impurities followed by several times rinsing with deionized water. The compound was then slowly melted to isotropic state on the silicon and allowed to flow through these channels and cooled down very slowly to observe the alignment of the compound.

Results and Discussion

Triphenylenes or phthalocyanines bearing an alkoxy group at or within their periphery are smaller discotic systems and spontaneously align homeotropically when they are slowly allowed to cool from the isotropic state.[38,39] However, the molecules of TPAD-12, with several possible conformations (due to the presence of different linking groups, viz. imine and ester) and steric hindrance (due to a high percentage of alkyl chains), can orient in space in several ways. Thus, these molecules do not arrange homeotropically simply by slow cooling. Therefore, on slow cooling from isotropic melt TPAD-12 molecules align parallel to the surface (edge on) on an untreated glass plate and exhibit an optical texture with developable domains[57,58] as observed under polarizing optical microscopy (POM) is shown in Figure 4a. To achieve the homeotropic alignment of the molecules, there is a need to increase the strength of the surface anchoring with the aromatic core of the disk. Surface anchoring can be enhanced by the formation of spin-coated thin as well as thick films prepared from solution by evaporation either on ITO or polyimide-coated glass plates. The spin-coated films (both thin and thick) thus appeared completely black, under polarized optical microscopy as shown in Figure 4b, reflecting the uniform alignment of the molecules on the substrate and uniform strength of surface anchoring with polar surface. The thickness of the film is much less than in Figure 4a. This indicates that discotic columns are aligned perpendicular to the substrate surface, and the columnar axis is parallel to the axis of polarized light. However, when the spin-coated film (Figure 4b) was heated to isotropic phase, the anchoring of the columns with the surface promoted by spin-coating is lost due to random ordering. When the film cooled to liquid crystalline phase, the anchoring is vanished and the formation of the edge-on orientation of the molecules was easily evidenced by the induced birefringent texture observed between

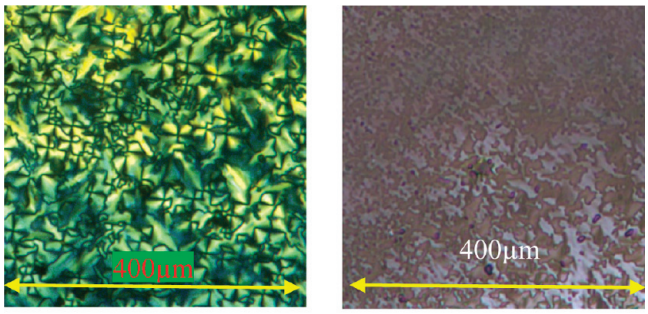

Figure 5. Optical texture in (a) absence of magnetic field and (b) presence of magnetic field.

the cross polarizers (Figure 4c). The surface anchoring with TPAD-12 molecules established by spin-coating gradually decreases with the increasing temperature and completely vanishes on going to isotropic liquid phase. Again, on cooling the isotropic melt, the surface anchoring duly promoted by spin-coating in virgin sample is lost and hence could not hold the columns of TPAD-12 molecules perpendicular to substrate. It has been reported that at the same cooling rate homeotropic alignment is favored in relatively thick samples (>300 or 400 nm) whereas planar alignment favored in thin cells.[59] Keeping this in mind, when a thick film was produced on the same substrate by spin-coating, defects appeared on both the substrates even before heating. There is some critical thickness above which the governing influence of the surface layer is lost within the bulk of the film or at the surface; thereby random columnar growth became dominant.[37] Furthermore, the end of the columns is highly unfavorable when exposed to air.[59]

Hence, two types of cells are fabricated one with ITO-coated glass plates and the other with PI-coated glass plates with a cell gap of 6 μm to remove the air−surface interaction. When these cells were filled up by the compound by capillary action from isotropic melt instead of spin-coating and cooled to the mesophase at different rates of cooling, viz., 0.1 and 10 °C/min, developable defects were observed in both cases, and the defects appeared similar to those that appeared in normal glass and cover slide cell. Thus, in both techniques, coating a surface of the substrate and adjusting the rate of the cooling could not produce the homeotropic alignment.

Magnetic alignment is one of the most straightforward and efficient methods to produce molecular materials ordered over bulk scales in almost all circumstances. The discotic liquid crystals exhibit a negative diamagnetic anisotropy, and hence the columnar director preferably aligns perpendicular to the applied magnetic field.[23,60] A 6 μm thick cell was used for magnetic alignment, and the cell was placed in a magnetic field of 2 T and heated to isotropic and cooled very slowly at the rate of 0.1 °C/min up to room temperature. But even 2 T magnetic field could not fully align this columnar phase perpendicular to the substrate because the defects as shown in Figure 5 appeared when observed under the cross polarizer.

Microchannel Experiment.[52] In order to ascertain the importance of surface anchoring on the molecular alignment, the compound was cooled down from isotropic liquid; we observed the developable defects in the microchannel as shown in Figure 6a, which is not regular and almost identical to those textures observed in normal thin film of the glass plate and coverslip. Hence, the microchannel experiment also does not hold promise to obtain a uniform homeotropic alignment of TPAD-12.

Finally, we have used a nanoelectrode as a substrate for the alignment of the columns of the TPAD-12 molecules. When a thin layer of SWNT is coated on the glass surface, LCs tend to assemble into an ordered microscopic structure.[61] SWNTs can be readily assembled on the glass substrate in a periodic pattern which can lead to a three-dimensionally ordered structure.[62] This ordered structured is advantageous to support the column of the discotic molecule when they immersed from the isotropic liquid. Introduction of SWNT into the columnar matrix does not destroy the mesophase of the host DLC.[63,64] Here we used this alignment technique in a reverse manner. A thin layer of the SWNT was deposited on the normal glass plate to make a uniform conductive layer which looks transparent when held against white light. A dilute solution (3.7 mg in 300 μL) of TPAD-12 was spin-coated on top of the SWNT electrode surface. These films appear completely black under the microscope (Figure 7a), which indicated that the columns are aligned perpendicular to the electrode surface. Further the film was heated to the isotropic phase followed by the immediate removal of the glass plate from the hot stage, then kept in the ice chamber for few minutes, and slowly allowed the temperature to rise up to 25 °C. After annealing the film further for few hours at 25 °C, the film appeared completely homeotropic as shown in Figure 7b. During crystallization from isotropic phase the molecules first arrange "face-on" toward the substrate, providing the necessary seed for the homeotropic growth of other molecules. Furthermore, the face-on arrangement was favored by the slow cooling from isotropic phase to mesophase or maintaining the thermal equilibrium at isotropic−mesophase transition for few hours.[38] But the high order interaction between the polar electrode surface with the aromatic cores and the polar

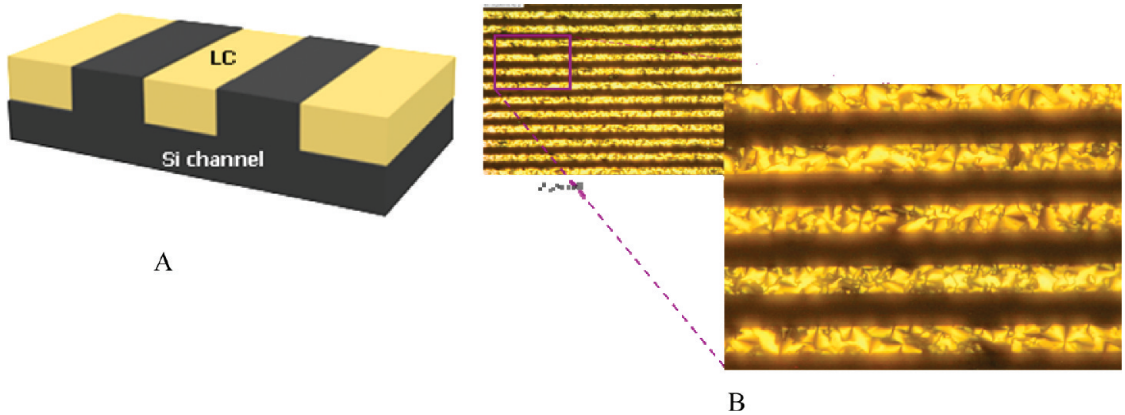

Figure 6. (A) Schematic representation of space filling of the LC compound in the confined microchannel. (B) Texture observed in 20 μm microchannel after cooling from isotropic phase.

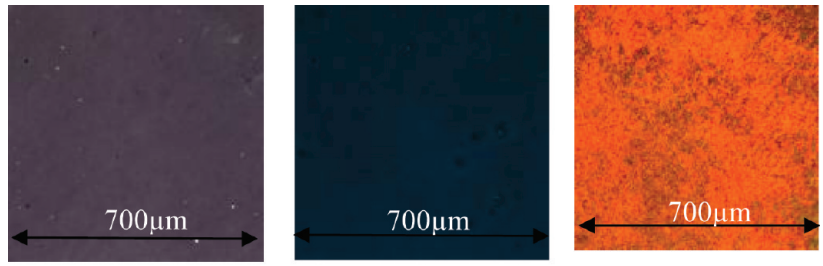

Figure 7. Optical microphotograph of nanoelectrode substrate spin-coated with TPAD-12 (a) before heat, (b) after heat, and (c) 6 μm thick cell of nanoelectrode filled by the capillary method.

linking groups (comprising of ether and imine linkages) in the side chain promotes the column to stand perpendicular to the substrate and freeze due to sudden drop in temperature. This interaction is so strong that even at 1 μm thickness the film remained homeotropic unlike the ITO- and polyimide-coated substrates. This is because as the film grows thicker, the governing influence of surface is still strong enough to hold the column perpendicular to the substrate even at 1 μm thick film and retain the homeotropic alignment. However, when TPAD-12 was filled up into a cell comprised of two nanoelectrodes having thickness of 6 μm by the capillary action from isotropic melt and immediately cooled down on ice, the film appeared (Figure 7c) uniform and highly colored without any defect line, indicating the retention of partial columnar homeotropic alignment and partial planar alignment. Hence, the surface anchoring by the SWNT electrode as well as the spin-coating of the sample on the substrate plays an important role in the homeotropic alignment of TPAD-12. Further the interaction between the discotic molecules with the SWNT electrode surface formed by spin-coating is strong enough to retain the face on arrangement even after rapid thermal quenching even at 1 μm thick film which is not observed on any other coated surface. Contact mode AFM studies[65] carried out on the surface morphology of the quenched discotic mesophase, exhibited by polymerizable 2-[(3,6,7,10,11-pentabutoxy-1-nitro-2-triphenylenyl)oxy]ethyl acrylate, in 50−100 nm thin films on highly oriented pyrolytic graphite (HOPG)−solution interface revealed the homeotropic molecular level ordering. The close-packed columns of triphenylene molecules are oriented parallel to the surface normal direction; the molecules are hence oriented with their planes in the plane of the HOPG substrate. This face-on orientation is in contrast to the observed edge-on orientation in self-assembled monolayers (SAMs) on gold[66] or thin films obtained by Langmuir−Blodgett (LB) techniques.[67]

Atomic Force Microscopy Studies on Thin Films. Columnar liquid crystals comprised with aromatic disks assemble into columnar stacks and found to exhibit excellent charge transport properties along the columns, which has led to very promising proof-of-principle photovoltaic cell.[1,13,20,68,69] Porphyrin-based discotic liquid crystals are also found to be prime candidates[70−72] for photovoltaic devices. The homeotropically aligned discotic columnar phases can conduct the charge particles efficiently in the correct direction toward the electrode surface. TPAD-12 is found to retain the columnar phase even at room temperature, and further it can be aligned homeotropically in thick films of the order of 1−3 μm by spin-coating. AFM studies were carried out to investigate the surface morphological characteristics and the suitability of these thin films for such applications. The solution of TPAD-12 in toluene was spin-coated on plasma-cleaned silicon substrate (SiO_2) to obtain thin films of TPAD-12 silicon substrate. The film thickness was monitored by ellipsometry and found to be 38 nm. The reflection image of the film is shown in Figure 8a. Though the film looks uniform there are some bright spots which appeared due to cluster formation of the compound solidified during spin-coating. The examination of surface profiles in the two regions, i.e., uniform region and bright spot regions, revealed the following features. The surface profile of the marked square area is displayed in Figure 8b, and it appeared uniform in the marked area. Such smooth appearance of surface is found to be due to ordered homeotropic alignment of the columns of DLC.[22] The AFM study on the bright spot area of the film shown in Figure 8c revealed that surface of the cluster has a circular wavelike pattern with vertical height of 200 nm with variable diameter of 10−20 μm. Such a typical pattern is formed, reflecting the accumulation of molecules with random ordering, due to slow spinning motion of the concentrated solution and rapid evaporation of the solvent from these areas. This random molecular arrangement interrupts the continuous charge migration from one electrode to the other through the column of DLC. However, the 2D AFM image of the uniform area of the film is shown in Figure 8d where the overall roughness is $R_q = 0.37$ nm. Hence, such small roughness demonstrated the homeotropic alignment of columns of TPAD-12 to promote the charge migration.

Polarization-Dependent Fluorescent Intensity, FCPM Studies. The molecular orientational patterns and 3-D imaging of director structures in thermotropic liquid crystals were investigated by the FCPM[45−48] to elucidate the structural information and fluorescent characteristics. In general, the confocal imaging technique is performed on the director field of the 3-D pattern of the dissolved fluorescent dye (concentration <0.01 wt %) in a nonfluorescent liquid crystal matrix to visualize the director field. However, the compound TPAD-12 exhibited fluorescence with Stokes shift of 160 nm.[40] Hence, we measured the anisotropy of fluorescent intensity driven by the chromophore by FCPM technique to determine the molecular arrangement in the discotic phase of the compound of the melt film sandwiched between a glass slide and a coverslip. Then the cell is excited with 488 nm argon laser, and the corresponding fluorescence image was observed on the monitor. We assume that the absorption/emission transition dipole orientations used to reveal molecular orientation patterns do not change among the smectic, columnar, and crystalline phases, and the emission dipole is parallel to the columnar axis. The anisotropic FCPM textures of *XY* and *XZ* optical slices taken from the middle plane of the thin film cell of TPAD-12 at room temperature are presented in Figure 9a−d. They revealed interesting optical phenomena of fan-shaped texture like real images and their polarizer-dependent fluorescence (Figure 9a,b) in two mutually perpendicular directions of polarizer and analyzer. When the polarization direction of the excitation light is parallel and perpendicular to the fan direction, the fluorescent intensity

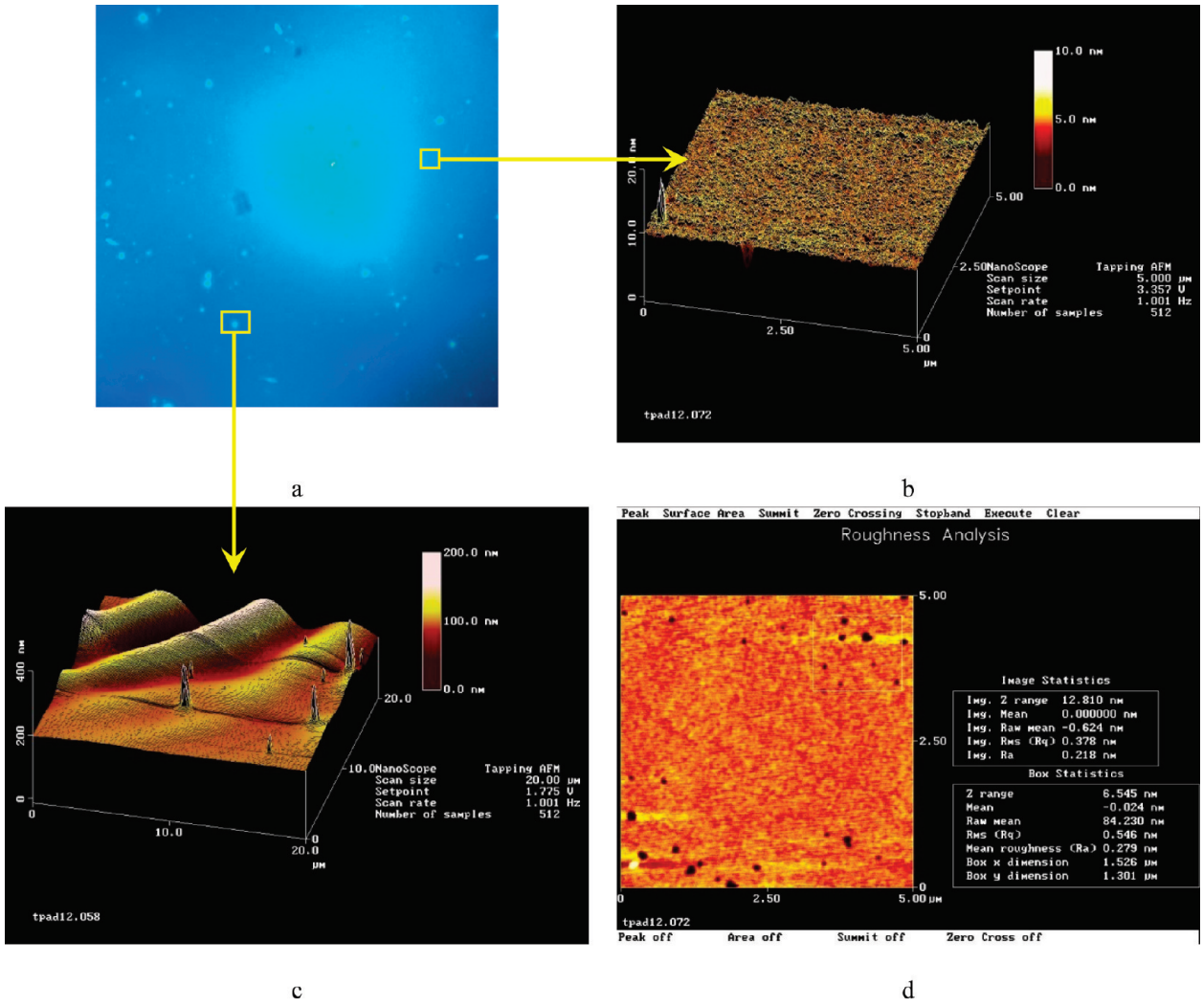

Figure 8. (a) Reflection image of spin coated TPAD-12 on silicon substrate. (b) AFM topography image of TPAD-12 showing uniform surface morphology. (c) Roughness analysis of uniform surface of TPAD-12. (d) Surface morphology of the cluster showing circular wavelike pattern.

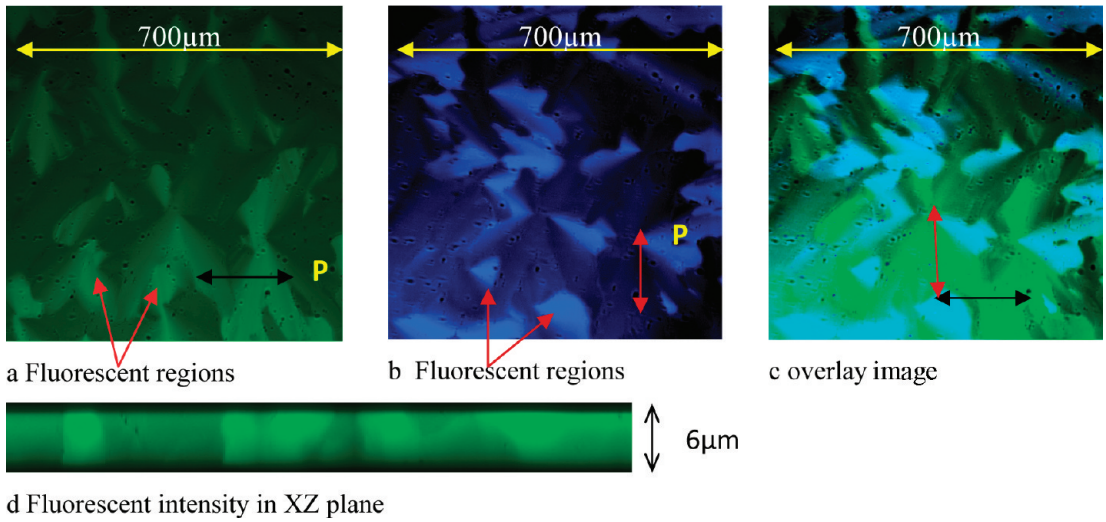

Figure 9. FCPM images of texture exhibited by of TPAD-12 at 25 °C: (a) *XY* optical slice from the middle plane of the cell with the polarizer in the *X* direction; (b) same as in (a) with the analyzer in *Y* direction; (c) overlay texture of (a), and (c, d) optical image exhibited by *XZ* optical slice inferring with defects in the entire volume of the cell.

becomes weaker and stronger, respectively. One can distinguish the dark and bright active regions of fluorescence with the polarizer in horizontal and vertical directions, respectively, as shown in Figure 9a,b. Adjacent bright regions can be clearly seen when shown using different colors in the overlay image of Figure 9c, and the images obtained (Figure 9a−c) demonstrated that the confocal fluorescence images of the columnar phase can be obtained without a dye dopant. The developable

domains are clearly observed and agree well with those observed in the polarizing optical microscope. The defect which is appearing on the surface of the columnar phase actually grows deep inside the whole film, and further studies of the vertical cross sections via FCPM scanning of the sample at different depths of the film, as shown in Figure 9d, also confirmed the fluorescence in the entire volume element rather than only on the surface. Hence, the fluorescence property of TPAD-12 is a bulk property and not a surface phenomenon of the molecules.

Conclusions

In summary, among the different substrates studied in this work, efficient homeotropic alignment of TPAD-12 was best observed by spin-coating on the SWNT-coated substrate. The strength of interaction of the SWNT electrode surface with the aromatic core of the disk like molecules is very important to promote the homeotropic alignment even for thick samples of the order of 1 μm. This alignment was retained even at repeated heating and cooling cycles. Further, the presence of ester and imine polar groups in the discotic molecule may explain the affinity toward molecular face-on anchoring on these surfaces initially since such groups contribute to the reduction of surface tension between the discotic molecules and the substrate interface. Spin-coating also plays an important role in inducing the surface anchoring, while sample injection of isotropic liquid by capillary action in to the electrode cell did not promote the homeotropic alignment totally. Thus, spin-coated film sandwiched between the two nanoelectrodes will produce a complete homeotropic cell, and such a cell can be a good candidate for photovoltaic application. It is noteworthy that PTFE nanopatterned glass substrates[22] also promote homeotropic alignment in hexagonal columnar phases exhibited by different chemical structures. In the present case, the molecules are pyramid-like and the interactions between alkyl chains of the core surrounding the apex and nanocarbon structures induce homeotropic alignment.

Acknowledgment. This research was supported by the International Institute for Complex Adaptive Matter (I2CAM) exchange award program as well as by DST, DAE, DRDO, and UGC in India and the NSF grants DMR 0645461, DMR-0820579, and DMR-0847782 in the USA.

References and Notes

(1) Schmidt-Mende, L.; Fechtenkotter, A.; Mullen, K.; Moons, E.; Friend, R. H.; MacKenzie, J. D. *Science* **2001**, *293*, 1119.

(2) Hoogboom, J.; Elemans, J. A. A. W.; Rasing, T.; Rowan, A. E.; Nolte, R. J. M. *Polym. Int.* **2007**, *56*, 1186.

(3) Hoogboom, J.; Behdani, M.; Elemans, J. A. A. W.; Devillers, M. A. C.; Gelder, de R.; Rowan, A. E.; Rasing, T.; Nolte, R. M. *Angew. Chem., Int. Ed.* **2003**, *42*, 1812.

(4) Percec, V.; Glodde, M.; Bera, T. K.; Miura, Y.; Shiyanovskaya, I.; Singer, K. D.; Balagurusamy, V. S. K.; Heiney, P. A.; Schnell, I.; Rapp, A.; Spiess, H. W.; Hudson, S. D.; Duan, H. *Nature* **2002**, *419*, 384.

(5) Feng, X.; Marcon, V.; Pisula, W.; Hansen, M. R.; Kirkpatrick, J.; Grozema, F.; Andrienko, D.; Kremer, K.; Mullen, K. *Nature Mater.* **2009**, *8*, 421.

(6) Gregg, B. A.; Fox, M. A.; Bard, A. J. *J. Phys. Chem.* **1990**, *94*, 1586.

(7) Bunk, O.; Nielsen, M. M.; Solling, T. I.; van de Craats, A. M.; Stutzmann, N. *J. Am. Chem. Soc.* **2003**, *125*, 2252.

(8) Van de Craats, A. M.; Stutzmann, N.; Bunk, O.; Nielsen, M. M.; Watson, M.; Mullen, K.; Chancy, H. D.; Sirringhaus, H.; Friend, R. H. *Adv. Mater.* **2003**, *15*, 495.

(9) McCulloch, I.; Heeney, M.; Bailey, C.; Genevicius, K.; MacDonald, I.; Shkunov, M.; Sparrowe, D.; Tierney, S.; Wagner, R.; Zhang, W.; Chabinyc, M. L.; Kline, R. J.; McGehee, M. D.; Toney, M. F. *Nature Mater.* **2006**, *5*, 328.

(10) Engelkamp, H.; Nolte, R. J. M. *J. Porphyrins Phthalocyanines* **2000**, *4*, 454.

(11) Matharu, A. S.; Jeeva, S.; Ramanujam, P. S. *Chem. Soc. Rev.* **2007**, *36*, 1868.

(12) Goodby, J. W. *Chem. Soc. Rev.* **2007**, *36*, 1855.

(13) Sergeyev, S.; Pisula, W.; Geerts, Y. H. *Chem. Soc. Rev.* **2007**, *36*, 1902.

(14) Kato, T. *Science* **2002**, *295*, 2414.

(15) Leclere, P.; Surin, M.; Henze, O.; Jonkheijm, P.; Biscarini, F.; Cavallini, M.; Feast, W. J.; Kilbinger, A. F. M.; Lazzaroni, R.; Meijer, E. W.; Schenning, A. P. H. J. *J. Mater. Chem.* **2004**, *14*, 1959.

(16) Melucci, M.; Barbarella, G.; Zambianchi, M.; Biscarini, F.; Cavallini, M.; Bongini, A.; Mazzeo, M.; Gigli, G. *Macromolecules* **2004**, *37*, 5692.

(17) Leclere, P.; Surin, M.; Cavallini, M.; Biscarini, F.; Lazzaroni, R. *Mater. Sci. Eng. R.* **2006**, *55*, 1.

(18) Kumar, S. *Chem. Soc. Rev.* **2006**, *35*, 83.

(19) Laaschat, S.; Baro, A.; Steinke, N.; Giesselmann, F.; Hagele, C.; Scalia, G.; Judele, R.; Kapatsina, E.; Sauer, S.; Schreivogel, A.; Tosoni, M. *Angew. Chem., Int. Ed.* **2007**, *46*, 4832.

(20) Adam, D.; Schumacher, P.; Simmerer, J.; Haussling, L.; Siemensmeyer, K.; Etzbach, K. H.; Ringsdorf, H.; Haarer, D. *Nature* **1994**, *371*, 141.

(21) Boden, N.; Bushby, R. J.; Clements, J.; Movaghar, B.; Donovan, K. J.; Kreouzis, T. *Phys. Rev. B* **1995**, *52*, 13274.

(22) Gearba, R. I.; Anokhin, D. V.; Bondar, A. I.; Bras, W.; Jahr, M.; Lehmann, M.; Ivanov, D. A. *Adv. Mater.* **2007**, *19*, 815.

(23) Lee, J. H.; Kim, H. S.; Pate, B. D.; Choi, S. M. *Physica B* **2006**, *798*, 385.

(24) Jung, J.; Rybaka, A.; Slazak, A.; Bialecki, S.; Miskiewicz, P.; Glowacki, I.; Ulanski, J.; Rosselli, S.; Yasuda, A.; Nelles, G.; Tomovic, Z.; Watson, M. D.; Mullen, K. *Synth. Met.* **2005**, *155*, 150.

(25) Monobe, H.; Hori, H.; Heya, M.; Awazu, K.; Shimizu, Y. *Thin Solid Films* **2006**, *499*, 259.

(26) Ichimura, K.; Furumi, S.; Morino, S.; Kidowaki, M.; Nakagawa, M.; Ogawa, M.; Nishiura, Y. *Adv. Mater.* **2000**, *12*, 950.

(27) Bonosi, F.; Ricciardi, G.; Lelj, F.; Martini, G. *J. Phys. Chem.* **1993**, *97*, 9181.

(28) Maliszewskyj, N. C.; Heiney, P. A.; Josefowicz, J. Y.; Plesnivy, T.; Ringsdorf, H.; Schuhmacher, P. *Langmuir* **1995**, *11*, 1666.

(29) Pisula, W.; Tomovic, Z.; Stepputat, M.; Kolb, U.; Pakula, T.; Mullen, K. *Chem. Mater.* **2005**, *17*, 2641.

(30) Tracz, A.; Makowski, T.; Masirek, S.; Pisula, W.; Geerts, Y. H. *Nanotechnology* **2007**, *18*, 485303.

(31) Misckiewicz, P.; Rybak, A.; Jung, J.; Glowacki, I.; Ulanski, J.; Geerts, Y. H.; Watson, M.; Mullen, K. *Synth. Met.* **2003**, *137*, 905.

(32) Furumi, S.; Janietz, D.; Kidowaki, M.; Nakagawa, M.; Morino, S.; Stumpe, J.; Ichimura, K. *Chem. Mater.* **2001**, *13*, 1434.

(33) Furumi, S.; Kidowaki, M.; Ogawa, M.; Nishiura, Y.; Ichimura, K. *J. Phys. Chem. B* **2005**, *109*, 9245.

(34) Lee, B. W.; Clark, N. A. *Science* **2001**, *291*, 2576.

(35) Eichhorn, S. H.; Adavelli, A.; Li, H. S.; Fox, N. *Mol. Cryst. Liq. Cryst.* **2003**, *397*, 347.

(36) Cavallini, M.; Calo, A.; Stoliar, P.; Kengne, J. C.; Martins, S.; Matacotta, F. C.; Quist, F.; Gbabode, G.; Dumont, N.; Geerts, Y. H.; Biscarini, F. *Adv. Mater.* **2009**, *21*, 4688.

(37) Schweicher, G.; Gbabode, G.; Quist, F.; Debever, O.; Dumont, N.; Sergeyev, S.; Geerts, Y. H. *Chem. Mater.* **2009**, *21*, 5867.

(38) Pisula, W.; Tomovic, Z.; El Hamaouki, B.; Watson, M. D.; Pakula, T.; Mullen, K. *Adv. Funct. Mater.* **2005**, *15*, 893.

(39) Terasawa, N.; Monobe, H.; Kiyohara, K.; Shimizu, Y. *Chem. Commun.* **2003**, 1678.

(40) Majumdar, K. C.; Pal, N.; Debnath, P.; Rao, N. V. S. *Tetrahedron Lett.* **2007**, *48*, 6330.

(41) Wang, Y. J.; Sheu, H. S.; Lai, C. K. *Tetrahedron* **2007**, *63*, 1695.

(42) Balakrishnan, K.; Datar, A.; Zhang, W.; Yang, X.; Naddo, T.; Huang, J.; Zuo, J.; Yen, M.; Moore, J. S.; Zang, L. *J. Am. Chem. Soc.* **2006**, *128*, 6576.

(43) Yip, H. L.; Zou, J.; Ma, H.; Tian, Y.; Tucker, N. M.; Jen, A. K. Y. *J. Am. Chem. Soc.* **2006**, *128*, 13042.

(44) Zucchi, G.; Viville, P.; Donnio, B.; Vlad, A.; Melinte, S.; Mondeshki, M.; Graf, R.; Spiess, H. W.; Geerts, Y. H.; Lazzaroni, R. *J. Phys. Chem. B* **2009**, *113*, 5448.

(45) Smalyukh, I. I.; Termine, D. J.; Shiyanovskii, S. V.; Lavrentovich, O. D. *G.I.T. Imag. Microsc.* **2001**, *3*, 16.

(46) Shiyanovskii, S. V.; Smalyukh, I. I.; Lavrentovich, O. D. In *Defects in Liquid Crystals: Computer Simulations, Theory and Experiment*; Lavrentovich, O. D., Pasini, P., Zannoni, C., Zumer, S., Eds.; Kluwer Academic Publishers: Amsterdam, 2006; Chapter 10, p 229.

(47) Smalyukh, I. I.; Shiyanovskii, S. V.; Lavrentovich, O. D. *Chem. Phys. Lett.* **2001**, *88*, 336.

(48) Smalyukh, I. I. *Mol. Cryst. Liq. Cryst.* **2007**, *23*, 477.

(49) Kachynski, A. V.; Kuzmin, A. N.; Prasad, P. N.; Smalyukh, I. I. *Appl. Phys. Lett.* **2007**, *91*, 151905; *Opt. Express* **2008**, *16*, 10617.

(50) Saar, B. C.; Park, H. S.; Xie, X. S.; Lavrentovich, O. D. *Opt. Express* **2007**, *15*, 13585.

(51) (a) Chen, B. C.; Lim, S. H. *Appl. Phys. Lett.* **2009**, *94*, 171911. (b) Lee, T.; Trivedi, R. P.; Smalyukh, I. I. *Opt. Lett.* **2010**, *35*, 3447–3449. (c) Lee, T.; Trivedi, R. P.; Bertness, K.; Smalyukh, I. I. *Opt. Express* **2010**, *18*, 27658–27669.

(52) Yoon, D. K.; Choi, M. C.; Kim, Y. H.; Kim, M. W.; Lavrentovich, O. D.; Jung, H. T. *Nature Mater.* **2007**, *6*, 866.

(53) Kim, Y. H.; Doon, D. K.; Choi, M. C.; Jeong, H. S.; Kim, M. W.; Lavrentovich, O. D.; Jung, H. T. *Langmuir* **2009**, *25*, 1685.

(54) Choi, M. C.; Pfohl, T.; Wen, Z. Y.; Li, Y. L.; Kim, M. W.; Israelachvili, J. N.; Safinya, C. R. *Proc. Natl. Acad. Sci. U.S.A.* **2004**, *101*, 17340.

(55) Tenent, R. C.; Barnes, T. M.; Bergeson, J. D.; Ferguson, A. J.; To, B.; Gedvilas, L. M.; Heben, M. J.; Blackburn, J. L. *Adv. Mater.* **2009**, *21*, 3210.

(56) Madou, M. J. *Fundamentals of Microfabrication*; CRC Press: Boca Raton, FL, 2002.

(57) (a) Hartshorn, N. H. *The Microscopy of Liquid Crystals*; Microscope Publications: London, 1974. (b) Chandrasekhar, S., *Liquid Crystals*, 2nd ed.; Cambridge University Press: Cambridge, 1992. (c) Meyer, C.; Cunff, L. L.; Belloul, M.; Foyart, G. *Materials* **2009**, *2*, 499.

(58) Oswald, P.; Pieranski, P. *Smectic and Columnar Liquid Crystals*; CRC Press: Boca Raton, FL, 2006.

(59) Grelet, E.; Bock, H. *Europhys. Lett.* **2006**, *73*, 712.

(60) Lee, J. H.; Choi, S. M.; Pate, B. D.; Chisholm, M. H.; Han, Y. S. *J. Mater. Chem.* **2006**, *16*, 2785.

(61) Ulman, A. *An Introduction to Ultrathin Organic Films: From Langmuir Blodgett to Self Assembly*; Academic Press: San Diego, CA, 1991.

(62) Shimoda, H.; Oh, S. J.; Geng, H. Z.; Walker, R. J.; Zhang, X. B.; McNeil, L. E.; Zhou, O. *Adv. Mater.* **2002**, *14*, 899.

(63) Bisoyi, H. K.; Kumar, S. *J. Mater. Chem.* **2008**, *18*, 3032.

(64) Kumar, S.; Bisoyi, H. K. *Angew. Chem., Int. Ed.* **2007**, *46*, 1501.

(65) Schnherr, H.; Manickam, M.; Kumar, S. *Langmuir* **2002**, *18*, 7082.

(66) Schonherr, H.; Kremer, F. J. B.; Kumar, S.; Rego, J. A.; Wolf, H.; Ringsdorf, H.; Jaschke, M.; Butt, H. J.; Bamberg, E. *J. Am. Chem. Soc.* **1996**, *118*, 13051.

(67) Tsukruk, V. V.; Reneker, D. H.; Bengs, H.; Ringsdorf, H. *Langmuir* **1993**, *9*, 2141.

(68) Charlet, E.; Grelet, E.; Brettes, P.; Bock, H.; Saadaoui, H. *Appl. Phys. Lett.* **2008**, *92*, 024107.

(69) Bushby, R. J.; Lozman, O. R. *Curr. Opin. Colloid Interface Sci.* **2002**, *7*, 343.

(70) Kang, S. W.; Li, Q.; Chapman, B. D.; Pindak, R.; Cross, J. O.; Li, L.; Nakata, M.; Kumar, S. *Chem. Mater.* **2007**, *19*, 5657.

(71) Zhou, X.; Kang, S. W.; Kumar, S.; Kulkarni, R. R.; Cheng, S. Z. D.; Li, Q. *Chem. Mater.* **2008**, *20*, 3551.

(72) Li, L.; Kang, S. W.; Harden, J.; Sun, Q.; Zhou, X.; Dai, L.; Jakli, A.; Kumar, S.; Li, Q. *Liq. Cryst.* **2008**, *35*, 233.

JP106344F